

Scaling of the anomalous Hall effect in $\text{Sr}_{1-x}\text{Ca}_x\text{RuO}_3$

R. Mathieu^{*,†,1} A. Asamitsu^{†,1,2} H. Yamada,³ K. Takahashi,²
M. Kawasaki,^{3,4} Z. Fang,^{1,5} N. Nagaosa,^{2,3,6} and Y. Tokura^{1,2,3}

¹*Spin Superstructure Project (ERATO-SSS), JST, AIST Central 4, Tsukuba 305-8562, Japan*

²*Department of Applied Physics, University of Tokyo, Tokyo 113-8656, Japan*

³*Correlated Electron Research Center (CERC), AIST Central 4, Tsukuba 305-8562, Japan*

⁴*Institute for Materials Research, Tohoku University, Sendai 980-8577, Japan*

⁵*Institute of Physics, Chinese Academy of Science, Beijing 100080, China*

⁶*CREST, Japan Science and Technology Agency (JST)*

(Dated: February 21, 2019)

The anomalous Hall effect (AHE) of ferromagnetic thin films of $\text{Sr}_{1-x}\text{Ca}_x\text{RuO}_3$ ($0 \leq x \leq 0.4$) is studied as a function of x and temperature T . As x increases, both the transition temperature T_c and the magnetization M are reduced and vanishes near $x \sim 0.7$. For all compositions, the transverse resistivity ρ_H varies non-monotonously with T , and even changes sign, thus violating the conventional expression $\rho_H = R_o B + 4\pi R_s M(T)$ (B is the magnetic induction, while R_o and R_s are the ordinary and anomalous Hall coefficients). From the rather complicated data of ρ_H , we find a scaling behavior of the transverse conductivity σ_{xy} with $M(T)$, which is well reproduced by the first principle band calculation assuming the intrinsic origin of the AHE.

PACS numbers: 75.30.-m, 72.15.-v

It has been known that the Hall resistivity ρ_H in a ferromagnet¹ has some extra contribution originated from the spontaneous magnetization, which is assumed and often observed experimentally to be fitted by $\rho_H = R_o B + 4\pi R_s M$, where B is the magnetic induction and M is the magnetization of the material. $R_o B$ represents the ordinary Hall contribution, which is related to the nature and amount of charge carriers. It is a linear function of the applied magnetic field H as in the Hall measurement geometry, $B=H$. $R_s M$ is referred to as the anomalous Hall term, and is usually associated with the spin polarization of the conduction carriers and the relativistic spin-orbit interaction λ . According to the above definition of ρ_H , the anomalous Hall term is proportional to the magnetization of the material. Theoretically this relation has been derived in terms of the perturbative expansion in λ and M . However the quantitative analysis of the AHE has seldom been completed since its mechanism has not yet been established, and theories give much smaller values compared with the experiments. Furthermore, most of the theories regard the AHE as from extrinsic origins, involving processes such as skew scatterings and side-jump mechanisms^{1,2,3}. Therefore the magnitude of the AHE depends on the concentration and scattering strength of impurities, thermal spin-agitation, etc. In contrast to these conventional views, some recent works^{4,5,6,7} put more stress on the intrinsic mechanisms of AHE. Namely the phase of the Bloch wave-function in the momentum space determines the Hall conductivity σ_{xy} , which is largely determined by the band crossing points acting as “magnetic monopoles”⁸. As an explicit example, the AHE and magneto-optical effect of SrRuO_3 have been studied, and a good agreement was obtained between theory and experiments⁸. In the present paper, we report the extensive study of the AHE in $\text{Sr}_{1-x}\text{Ca}_x\text{RuO}_3$ ($0 \leq x \leq 0.4$) as a function of T and

x to reveal its systematics. We have found the scaling behavior of the transverse conductivity σ_{xy} in terms of the T - and x -dependence of the magnetization $M(x, T)$, which is in fairly good agreement with the first principle band calculation. This gives a firm evidence for the intrinsic origin of the AHE.

A fairly large spin orbit coupling exists in the ferromagnetic SrRuO_3 (SRO) metal. The $4d$ orbitals (Ru^{4+} ($t_{2g}^{\uparrow\uparrow\uparrow}, t_{2g}^{\downarrow}$)) are rather extended, and the Coulomb repulsion is small compared to the band width. The ferromagnetic properties of SRO are usually associated with a narrow itinerant band resulting from the hybridization between the $\text{Ru}(t_{2g})$ and $\text{O}(2p)$ orbitals. There are relatively few $4d$ metal oxides showing a long range ferromagnetic order (for example in comparison to the paramount number of $3d$ CMR manganites). Ruthenium oxides from the Ruddelston-Popper-type $\text{Sr}_{n+1}\text{Ru}_n\text{O}_{3n+1}$ series show metallic properties, as well as superconductivity and magnetic order⁹. SrRuO_3 ($n = \infty$, perovskite) is an itinerant ferromagnet^{10,11} with a Curie temperature (T_c) near 160 K in a single-crystal form. While similar structurally, and as well metallic, CaRuO_3 (CRO) does not exhibit ferromagnetism. The magnetic state of CaRuO_3 is still under discussion¹², but may correspond to a paramagnetic state with short range magnetic correlation, or to a system close to ferromagnetic instability¹³. In $\text{Sr}_{1-x}\text{Ca}_x\text{RuO}_3$, the ferromagnetic interaction becomes weaker with increasing x ¹⁴. For the compounds with larger Ca-doping ($x \geq 0.7$), no clear phase transition is discerned, and only some irreversibility is observed in the magnetization curves of these materials. As for CRO, the exact nature of the magnetic interaction observed in these samples is still under investigation¹⁵. The disappearance of the long range magnetic order is commonly related to the distortion of the RuO_6 octahedra associated with the partial or total replacement

of Sr by Ca, and the corresponding narrowing of the $4d$ bandwidth¹⁶.

$\text{Sr}_{1-x}\text{Ca}_x\text{RuO}_3$ polycrystalline ceramics have large electrical resistivities ($\sim 1\text{-}10\text{ m}\Omega\text{cm}$) associated with extrinsic contributions such as grain boundaries; they also show some degree of magnetic disorder and inhomogeneity. It is difficult to grow clean single crystals of Ca-doped SRO, although it is possible to prepare high quality single crystals of the end compounds, SRO and CRO. On the other hand, it is nowadays possible to grow high quality epitaxial films of SrRuO_3 and $\text{Sr}_{1-x}\text{Ca}_x\text{RuO}_3$ ($x \leq 0.5$)¹⁷. In the present article, we study the anomalous Hall resistivity of epitaxial films of $\text{Sr}_{1-x}\text{Ca}_x\text{RuO}_3$ ($0 \leq x \leq 0.4$), and its evolution as the ferromagnetic interaction decreases with x . The Hall resistivity contains an anomalous component, associated with the ferromagnetic ordering of the samples at low temperatures. This component is not simply proportional to the M , as usually assumed. The results reveal a close relation between σ_{xy} and the spin polarization of the system. Such a correlation was predicted by first principle calculations taking account of the spin-orbit interaction in terms of the Berry phase connection⁸. The calculations successfully reproduce the non-monotonous variation of σ_{xy} with temperature (via its magnetization), as well as its sign change. The effects of disorder and structural changes on the anomalous conductivity are discussed.

Thin ($\sim 500\text{ \AA}$) films of $\text{Sr}_{1-x}\text{Ca}_x\text{RuO}_3$ ($x = 0, 0.1, 0.2, 0.3, \text{ and } 0.4$) were epitaxially grown on the (001) surfaces of SrTiO_3 single-crystal substrates by pulsed laser deposition (PLD). Bulk single crystal SrRuO_3 (SRO) and CaRuO_3 (CRO) were prepared using a flux method for comparison. The quality of the films and phase-purity of the single crystals were confirmed by x-ray diffraction. Both single crystals have orthorhombic structure; SrRuO_3 has a relatively small orthorhombicity ($c/a=1.003$, $c/b=0.996$), while it is larger for CaRuO_3 ($c/a=1.01$, $c/b=0.980$). The epitaxial thin films are coherently strained by the SrTiO_3 substrate, yielding a tetragonal distortion in the [001] direction ($c/a=c/b=1.01$ for $x=0$). As a result, the out-of-plane lattice constants of the films are elongated (c.f. inset of Fig. 1), and due to the spin-orbit interaction, the easy axis of magnetization is perpendicular to the film plane. Magnetic and transport measurements were performed on the $\text{Sr}_{1-x}\text{Ca}_x\text{RuO}_3$ thin films and the single crystals of SRO and CRO. The magnetization data was recorded on a MPMS5S SQUID magnetometer using a magnetic field applied normal to the plane of the films. The films were then patterned in a six-lead Hall bar geometry using conventional photo-lithography and Ar ion etching for transport measurements. The Hall resistivity ρ_H was measured with a PPMS6000 system together with the longitudinal resistivity $\rho_{xx} = \rho$ as a function of H and T . The anomalous resistivity ρ_{xy} was extrapolated to $H = 0$ from ρ_H vs H measurements up to $H = 9\text{ T}$ at constant temperatures (2 K, 5 K, and from 10 K to 200 K in steps of 10 K) after subtraction of the ordinary

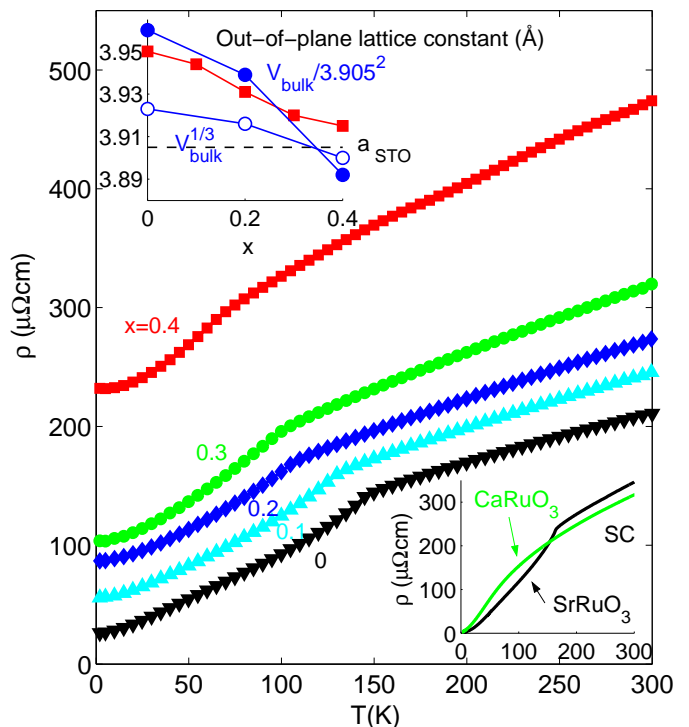


FIG. 1: (color online) Temperature dependence of the resistivity of the $\text{Sr}_{1-x}\text{Ca}_x\text{RuO}_3$ films (main frame) and single crystals of SrRuO_3 and CaRuO_3 (lower inset). The upper inset shows the variation of the out-of-plane lattice parameter of the films (squares). The lattice parameter of the SrTiO_3 substrate a_{STO} is indicated, as well as the average lattice parameter obtained for powders, for $a=b=c$ ($V^{1/3}$, V is the unit cell volume), and for a perfect elastic strain (Poisson ratio of 0.5; V/a_{STO}^2). The parameters of $x = 0, 0.1, \text{ and } 0.2$ ideally lie between the $V^{1/3}$ and V/a_{STO}^2 values; the small deviation observed from $x = 0.3$ and 0.4 may be related to a minor Ru deficiency; ruthenium oxides are very robust against oxygen deficiencies, so that the oxygen content should be stoichiometric.

(linear as a function of H) Hall contribution, and the transverse conductivity σ_{xy} was estimated as $-\rho_{xy}/\rho_{xx}^2$. Polycrystalline samples of $\text{Sr}_{1-x}\text{Ca}_x\text{RuO}_3$ were also prepared to check the variation of T_c with the Ca content. First-principles calculations of σ_{xy} were performed assuming orthorhombic and cubic crystal structures. The plane-wave pseudo-potential calculations were performed based on the local spin density approximation (LSDA), and the spin-orbit coupling was treated self-consistently by using the relativistic fully separable pseudo-potentials in the framework of non-collinear magnetism formalism. The finite life-time broadening was estimated from the experimental residual resistivity and the extended Drude analysis of the longitudinal conductivity¹⁸.

All the investigated samples are metallic as seen in Fig. 1 and inset. The residual resistivity at low temperatures is very low ($\sim 2.5\text{ }\mu\Omega\text{cm}$) for the single crystals, and increases for the films from 26 ($x = 0$) to 232 $\mu\Omega\text{cm}$ ($x = 0.4$). A kink is observed in the resistivity

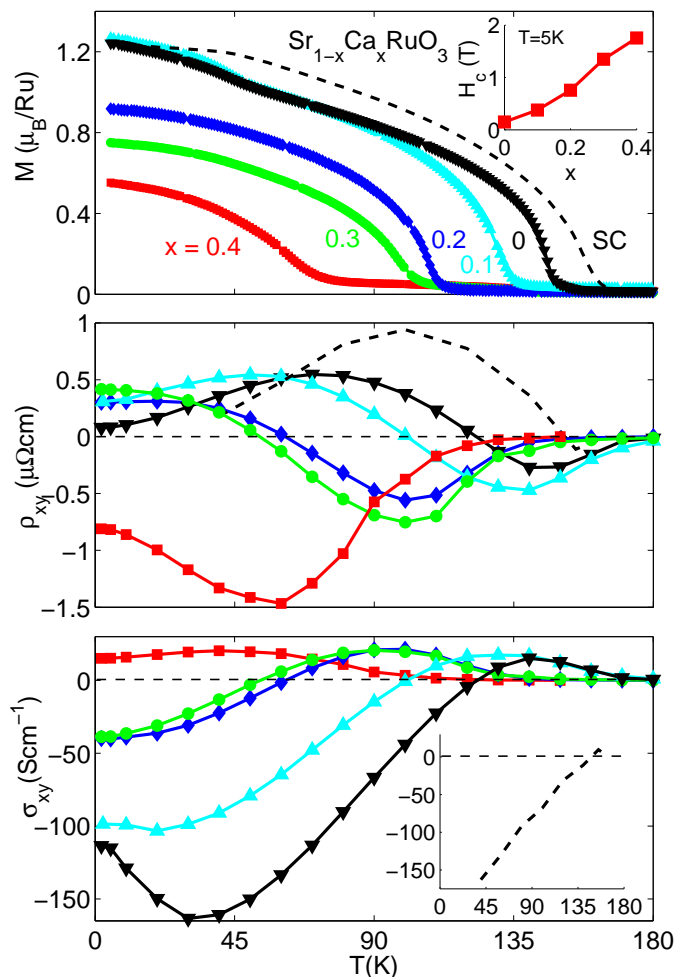


FIG. 2: (color online) Temperature dependence of the magnetization (top panel), transverse resistivity (middle panel), and transverse conductivity (bottom panel) of the $\text{Sr}_{1-x}\text{Ca}_x\text{RuO}_3$ films. In the SQUID experiments, the samples are cooled in $H = 7$ T, and the magnetization is recorded on re-heating in $H = 0.05$ T applied normal to the film planes. The results for the single crystal (SC) are included for comparison. The top inset shows the monotonous increase of the coercivity H_c with increasing Ca doping; $T = 5$ K.

curves, around the paramagnetic-to-ferromagnetic transition temperatures (T_c) of the films. No long range magnetic order is observed in CRO, and as seen in inset, the resistivity curve has no anomaly in the measured range of temperature. Due to the above mentioned strain effects, the epitaxial film of SRO has a slightly lower T_c than the single crystal, near 150 K^{19,20}. The substitution of Sr by Ca in $\text{Sr}_{1-x}\text{Ca}_x\text{RuO}_3$ weakens the ferromagnetic interaction, and T_c is greatly reduced. It is reduced to ~ 110 K for $x = 0.2$, and ~ 70 K for $x = 0.4$.

The top panel of Fig. 2 shows the temperature dependence of the 7 T-cooled magnetization of the films probed in a small field of $H = 0.05$ T applied normal to the plane, i.e. in the same direction as in the Hall measurements, along the easy axis of magnetization. As seen in inset, the

coercivity H_c of the films monotonously increases with increasing Ca doping. In addition to possible disorder, the Ca substitution yields structural changes, affecting the magnetic properties and, as we will discuss below, the AHE. At low temperatures, $M(H = 7$ T) amounts to $\sim 1.5 \mu_B/\text{Ru}$ for the undoped SRO film. Due to the itinerant character of the magnetism, the obtained moment is smaller than expected according to Hund's rule for Ru^{4+} in the $S = 1$ low spin state ($2 \mu_B/\text{Ru}$). $M(H = 7$ T) decreases with increasing Ca doping, and amounts to $\sim 0.75 \mu_B/\text{Ru}$ for $x = 0.4$. The middle panel of Fig. 2 shows the temperature dependence of the anomalous Hall resistivity ρ_{xy} for all the films and the SRO single crystal. At a constant temperature, ρ_H is a linear function of H at high fields, with a negative proportionality constant ($R_o < 0$), indicating charge carriers of electron-like nature. As seen

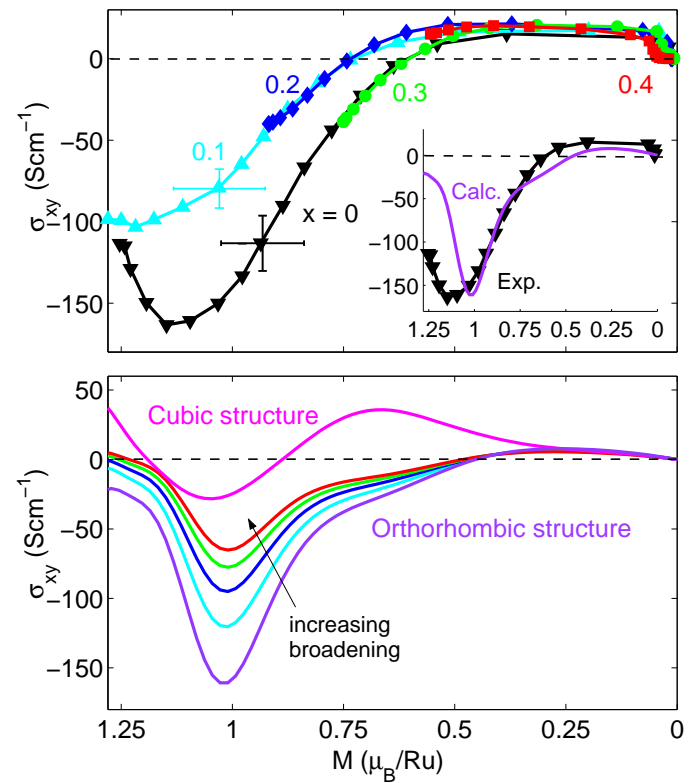


FIG. 3: (color online) Top panel: The transverse conductivity σ_{xy} data obtained for the films is plotted against the magnetization M , using the data from Fig. 2. Typical errors bars are indicated. As the areas of the films are well defined by patterning, the uncertainty on the magnitude of σ_{xy} is mainly determined by the error in thickness determination, which amounts to $\sim 5\%$ of the actual thickness. As a result, there is an uncertainty of $\sim 15\%$ on σ_{xy} (which is calculated from the ratio of ρ_{xy} and ρ_{xx}^2) and on an uncertainty of $\sim 5\%$ on the magnitude of M . Bottom panel: First principle calculations for cubic and orthorhombic structures. Results obtained using different broadening parameters are shown in the orthorhombic case.

in the figure, ρ_{xy} of the films varies non-monotonously with T . No AHE is observed at high temperatures. The

AHE appears just above T_c ; ρ_{xy} is negative, and show a maximum near T_c . At lower temperatures, ρ_{xy} changes sign (near 120 K for $x = 0$, and 60 K for $x = 0.2$), and remain positive down to the lowest temperature. For $x = 0.4$ with a lower T_c , however, the sign change is not observed. Similar features are observed for the single crystal of SRO²¹; the resistivity of the single crystals was too low below 40 K to estimate ρ_{xy} (and thus σ_{xy}). As seen in the bottom panel of Fig. 2, the anomalous conductivity remains fairly large at low temperatures, amounting to $\sim -100 \text{ Scm}^{-1}$ at 2 K for the undoped and $x = 0.1$ films. $\sigma_{xy}(T)$ shows a similar high-temperature peak, which, as T_c , is shifted to lower temperatures as the Ca doping increases. If the anomalous conductivity data in Fig. 2 is plotted against the magnetization instead of the temperature, as in the top of Fig. 3, one observes, within the measurement uncertainties, a similar or universal behavior of the Hall conductivity for all the samples. This indicates that the AHE is intrinsic to the system, and closely related to the spin polarization, which varies with T , as well as with x . First-principle calculations do show that the anomalous conductivity is very sensitive to the Fermi level position and the spin exchange-splitting⁸ and thus to the details of the band structure, including the population of these bands at a given temperature. The inset of Fig. 3 shows the results of the first-principle calculations for SRO (undoped case), using the orthorhombic structure obtained for the bulk SRO crystal⁸. As seen in this inset, the calculations reproduce closely the non-monotonous variation, as well as the sign change of σ_{xy} with M (or T). The first-principle calculations (bottom panel of Fig. 3) show how the anomalous Hall conductivity depends on the crystal structure and lifetime of the electrons. Results obtained by considering a cubic structure are indeed quite different from those obtained in the

orthorhombic case, even though they qualitatively show a similar non-monotonous behavior. It is also shown in the figure how the anomalous Hall conductivity is reduced upon increasing the scattering rate in the calculations; the broadening parameters were chosen so as to reflect the increase of longitudinal resistivity shown in Fig. 1. The Ca doping of the $\text{Sr}_{1-x}\text{Ca}_x\text{RuO}_3$ films also induces slight structural changes, such as a smaller orthorhombicity (or more correctly tetragonality, c.f. inset of Fig. 1). It is thus expected that the temperature dependence of σ_{xy} of the doped films should differ, more or less, from that of the undoped SRO film, reflecting the changes in the micro-structure of the system and their effect on the band structure. Nevertheless, if the additional electron scattering effects arising from the Ca doping are taken into account as the broadening-induced reduction of the magnitude of σ_{xy} , the anomalous Hall conductivity of the $\text{Sr}_{1-x}\text{Ca}_x\text{RuO}_3$ films shows a good scaling to M , while changing T and x . This indicates that the AHE is mainly of intrinsic origin, as described in terms of the Berry phase connection.⁸

In summary, the anomalous Hall effect was investigated for thin films of $\text{Sr}_{1-x}\text{Ca}_x\text{RuO}_3$, in which the ferromagnetic interaction is weakened with increasing Ca content x . The Hall resistivity of the films vary in a similar fashion with the temperature T . The obtained anomalous Hall conductivity varies non-monotonously and non-trivially with T , and even changes sign. The results however, show a good scaling solely to the T - and x -dependent magnetization M , which can be reproduced by first principles calculations. The anomalous Hall effect appears, as asserted by Fang et al⁸, as a hallmark of the presence of magnetic monopoles in the momentum space of the crystal.

Z.F. acknowledges the support from the NSF of China.

* roland@crc.u-tokyo.ac.jp

† Main address: Cryogenic Center, University of Tokyo, Tokyo 113-0032, Japan.

¹ R. Karplus and J. M. Luttinger, *Phys. Rev.* **95**, 1154 (1954); C. L. Chien and C. R. Westgate, *The Hall Effect and Its Applications*, Plenum Press, New York, (1979).

² J. M. Luttinger, *Phys. Rev.* **112**, 739 (1958); N. F. Mott and H. S. W. Massey, *Theory of Atomic Collisions*, Clarendon, Oxford, (1965).

³ P. Nozières and C. Lewiner, *J. Phys. (Paris)* **34**, 901 (1973).

⁴ J. Ye, Y. B. Kim, A. J. Millis, B. I. Shraiman, P. Majumdar, and Z. Tesanovic, *Phys. Rev. Lett.* **83**, 3737 (1999).

⁵ N. Nagaosa, *Mat. Sci. Eng. B* **84**, 58 (2001); Y. Taguchi, Y. Ohara, H. Yoshizawa, N. Nagaosa, and Y. Tokura, *Science* **291**, 2573 (2001).

⁶ Y. Lyanda-Geller, S. H. Chun, M. B. Salamon, P. M. Goldbart, P. D. Han, Y. Tomioka, A. Asamitsu, and Y. Tokura, *Phys. Rev B* **63**, 184426 (2001).

⁷ T. Jungwirth, Q. Niu, and A. H. MacDonald, *Phys. Rev. Lett.* **88**, 207208 (2002).

⁸ Z. Fang, N. Nagaosa, K. Takahashi, A. Asamitsu, R. Mathieu, T. Ogasawara, H. Yamada, M. Kawasaki, Y. Tokura, and K. Terakura, *Science* **302**, 92 (2003) and cond-mat/0310232.

⁹ As for example Sr_2RuO_4 and $\text{Sr}_3\text{Ru}_2\text{O}_7$; see: K. Ishida, H. Mukuda, Y. Kitaoka, K. Asayama, Z. Q. Mao, Y. Mori, and Y. Maeno, *Nature* **396**, 658 (1998); S.- I. Ikeda, Y. Maeno, S. Nakatsuji, M. Kosaka, and Y. Uwatoko, *Phys. Rev B* **62**, R6089 (2000).

¹⁰ A. Callaghan, C. W. Moller, and R. Ward, *Inorg. Chem.* **5**, 1572 (1966).

¹¹ P. B. Allen, H. Berger, O. Chauvet, L. Forro, T. Jarlborg, A. Junod, B. Revaz, and G. Santi, *Phys. Rev. B* **53**, 4393 (1996).

¹² N. Kolev, C. L. Chen, M. Gospodinov, R. P. Bontchev, V. N. Popov, A. P. Litvinchuk, M. V. Abrashev, V. G. Hadjiev, and M. N. Iliev, *Phys. Rev. B* **66**, 014101 (2002).

¹³ T. He and R. J. Cava, *Phys. Rev. B* **63**, 172403 (2001).

¹⁴ T. Kiyama, K. Yoshimura, K. Kosuge, H. Mitamura, and T. Goto, *J. Phys. Soc. Jpn.* **68**, 3372 (1999).

¹⁵ I. Felner and U. Asaf, *Physica B* **337**, 310 (2003).

- ¹⁶ G. Cao, S. McCall, M. Shepard, J. E. Crow, and R. P. Guertin, Phys. Rev. B **56**, 321 (1997).
- ¹⁷ C. B. Eom, R. J. Cava, R. M. Fleming, J. M. Phillips, R. B. van Dover, J. H. Marshall, J. W. P. Hsu, J. J. Krajewski, and W. F. Peck Jr., Science **258**, 1799 (1992).
- ¹⁸ See [8] as well as its corresponding *Supporting Online Material*.
- ¹⁹ Q. Gan, R. A. Rao, C. B. Eom, J. L. Garrett, and Mark Lee, Appl. Phys. Lett. **72**, 978 (1998).
- ²⁰ C. U. Jung, H. Yamada, M. Kawasaki, and Y. Tokura, unpublished.
- ²¹ In connection to [20], similar $\rho_{xy}(T)$ curves have also been obtained for other types of SRO films deposited on STO substrates with different orientations, or using buffer layers.